

The Total Energy in the Interaction of X-Ray Photons with Capacitors

¹ALOK RANJAN SAHU,

Gandhi Institute of Excellent Technocrats, Bhubaneswar

²SATYA NARAYAN SWAIN,

Orissa Engg College, Bhubaneswar

Abstract

Context and Background: In this research, we investigate the interaction of X-rays with a capacitor by studying the voltage established in the capacitor during the illumination. **Motivation:** We aim at verifying that the total energy conserved in the interaction is $P\tau$, i.e. the product of the average power P times the period τ of the X-rays. **Hypothesis:** Our investigation relies on the hypothesis that the voltage responsivity π_V of the capacitor should be small, according to previous research. The parameter π_V is the ratio between the voltage produced and the average power P of the X-rays, and measures the performance of the capacitor in response to the X-rays. **Method:** We measure the voltage produced by the capacitor in response to the X-rays, and then determine the average power P of the X-rays according to a procedure already assessed with infrared and visible light. **Results:** In our experiments, P turns out to be in the range between 10^{-3} W to 10^0 W. Our procedure enables us to unveil the relationship between the average power P and the effective dose, an important operating parameter used to measure the delivery of X-rays in practical applications, such as standard X-ray medical imaging machines. **Conclusions:** We believe that our procedure paves the way for designing a possible X-ray power-meter, a tool presently missing in the market of X-ray characterization tools.

Keywords: X-Rays, Power, Light-Matter Interaction, Conservation of Energy

1. Introduction

Our main research goal is to explore the interaction between electromagnetic (EM) waves and matter and to find a law capable of consistently and quantitatively explaining such interaction throughout the whole EM spectrum. Significant effort was spent in exploring the interaction of visible and infrared (IR) light with matter. Here we focus on the high frequency region of the EM spectrum, i.e. to X-rays, by applying and assessing in this region the same law of conservation of energy successfully tested in the visible and IR light regions.

Currently several questions remain without clear answer in considering phenomena related to the EM wave interaction with matter. How much is the total energy conserved in light-matter interaction? Usually, researchers respond adopting a microscopic point of view in which photons transfer their energy $h\nu$ (where h is Planck's constant and ν is the photon's frequency) to electrons or other charges. However, when EM waves interact with a macroscopic object such as a sensor, a detector, or an energy harvester, their energy $h\nu$ does not directly answer the question stated previously. Specifically, through $h\nu$ it becomes difficult to correlate the response (i.e. the voltage, current, or temperature change) of sensor, detector, or energy harvester, to the power, or the intensity, of the absorbed EM wave. Vice-versa, it is hard to associate the power or intensity of the EM wave to the magnitude of the electric currents producing them in an EM wave generator. This difficulty proposes several questions in diverse physical situations. For example, why, in response to dim light at an intensity of few $\text{mW}\cdot\text{m}^{-2}$ ($10^{-3} \text{ W}\cdot\text{m}^{-2}$), is the current generated in rod cells, or photoreceptors in the eye's retina, of the order of pA (10^{-12} A) [1]? Why, in the bulk photovoltaic effect with the absorption of IR light at $10.6 \mu\text{m}$ wavelength and 10 to 300 mW power, is the produced current of the order of μA (10^{-6} A) [2]? More generally, why is sensitivity steadily around 0.045 mA W^{-1} for photocurrents generated in different devices with red and IR light in the 1 to 200 mW power range [2] [3]? On the other hand, why, in free-electron-based

light sources, do electrons need to move close to the speed of light to emit ultraviolet (UV) light at a power of the order of only pW to nW (10^{-9} W) [4]? Finally, why, when illuminated by visible and IR light with power in the mW range, do capacitors with capacitance of the order of pF produce voltages in the mV range [5]?

Recent efforts provide a strategy to correlate the response (*i.e.* the voltage, current, or temperature change) of sensors, detectors and energy harvesters, to the power, or the intensity, of the absorbed EM waves. In these efforts, the law of conservation of energy is called into play [5]. Specifically, in absorption phenomena, the EM wave's total energy is matched to the energy transferred to the absorbing device (sensors, detectors, and energy harvesters). This match is effective when the total energy of the EM waves is expressed as the product of their average power P and their period τ , *i.e.* $P\tau$, as proven in the case of the absorption of IR and visible light by capacitors [5] [6]. Mathematical details are provided in the Appendix. Examples of the effectiveness of the approach based on $P\tau$ as the total energy are: the absorption of IR light by thin films in IR spectra [7], of visible light by the retina in vertebrate's vision [8], by molecules in photo-redox catalysis reactions [9], in photo-thermoelectric devices [9], and by neurons under two-photon excitation [9]. Vice-versa, in emission phenomena, $P\tau$ is effective in a number of cases. For example, one is high-order multiphoton Thomson scattering [10], where the collision of a near IR laser beam with relativistic electrons gives rise to X-rays. Another example is the quantification of the power of the anomalous microwave emission (AME) by spinning dust in the interstellar medium [11]. A third example is the estimation of the power emitted by radio waves produced in the interaction between a red dwarf and an exoplanet [12]. However, the effectiveness of $P\tau$ and the law of conservation of energy, expected to be valid in all manifestations of light-matter interaction, whether in absorption or in emission phenomena, is not yet assessed in the high frequency region of the EM spectrum, e.g. with X-rays. This assessment is the objective of this research.

We investigate the interaction of X-rays with a capacitor adopting a method similar to that in previous research [5]. Capacitors respond to visible and IR light through the production of a voltage with magnitude constrained by light's power P [5] [6]. The capacitors used in Refs. [5] and [6] are, actually, thermoelectric devices, whose multilayer structure mimics a capacitor with estimated capacitance C of the order of pF (10^{-12} F) [5] [6]. The ability of capacitors to respond to light is widely documented in nature. Indeed, natural capacitors, such as the retinal neuron cells, respond to visible light with voltage production depending upon light's power P [8]. Specifically, retinal neuron cells are compared to capacitors because their membrane acts as the capacitor's dielectric layer, while the intra- and extracellular conducting fluids, that flank the membrane, act as the capacitor's electrodes. The membrane's capacitance C is of the order of 6 - 8 pF [13]. Such order of magnitude of the capacitance is common: for instance, in the hippocampus of behaving mice, the magnitude of the neuron's capacitance is around 50 pF [14].

To assess the effectiveness of $P\tau$ and the law of conservation of energy in the absorption of X-rays by a capacitor, we first measure the voltage $\Delta V(t)$ produced versus time t by the capacitor, and then estimate the average power P of the X-rays through $P\tau$. Contemporarily, we collect the temperature $T_{\text{hot}}(t)$ generated on the capacitor's face exposed to the X-rays. This procedure is the same as that adopted in Ref. [5]. We then assess the value of the average power P by following two routes. The first consists of determining if the value of P complies with the performance of a standard X-ray medical machine and of an X-ray diffractometer. The second route consists of computing the voltage responsivity π_V of capacitors and comparing it to the value expected from the model based on $P\tau$. The voltage responsivity π_V measures the effectiveness of the capacitor's response to the EM waves, and is expected to increase with decreasing frequency ν (or with increasing period τ) of the EM waves [5]. We probe this trend of π_V with pulsed X-rays in a standard medical machine and continuous X-rays in a diffractometer. Finally, we discuss our findings.

2. Experimental Details

The X-ray sources: The main X-ray source we used in our experiment was originally designed for medical imaging. Therefore, we expect the performance of the X-ray source to be standard for medical imaging X-ray machines. The X-rays used in our experiment are 40 keV in energy, and are produced with a 10 mA source current. We used 40 kV to maximize the amount of absorbed beam. Indeed, at higher energies, much more of the X-ray energy would pass

through the capacitor, whereas at lower energy nearly all of it should be absorbed and the observed signal be above the background. In our set-up, the distance between the X-ray source and the capacitor is 90 cm, and the beam size is 4 cm^2 . The X-rays have a broad spectrum, however, given their 40 keV energy, we expect the X-rays to have a frequency ν centered around $9.65 \times 10^{18} \text{ Hz}$, and a period $\tau = \nu^{-1}$ centered around $0.104 \times 10^{-18} \text{ s}$. The average power of the X-rays is unknown, and estimating its value is one of the objectives of this research. We directed these X-rays normally to the capacitor's surface.

We also used Cu K- α and - β X-rays obtained from a powder X-ray diffractometer (PXRD) (X'pert PANalytical) with average wavelength $\lambda \sim 1.5406 \times 10^{-10} \text{ m}$, average frequency $\nu \sim 1.947 \times 10^{18} \text{ Hz}$, and average period $\tau \sim 0.51 \times 10^{-18} \text{ s}$. The beam size is 4 cm^2 . We directed also these X-rays normally to the capacitor's surface.

The Capacitors: The main capacitor used to test the interaction with X-rays is a stack of three Custom Thermoelectric 07111-9L31-04B modules. Each module has a length of $\approx 23 \text{ mm}$ along the x- and the y-axes, and a height $h = 3 \text{ mm}$. Moreover, each module is designed to produce a voltage difference ΔV when exposed to a temperature difference ΔT between the illuminated (T_{hot}) and non-illuminated (T_{cold}) faces. This effect is the Seebeck effect: $\Delta V = S \Delta T$, where S is the Seebeck coefficient and $\Delta T = T_{\text{hot}} - T_{\text{cold}}$. Finally, each module is a multi-layer of AlO-Cu-Bi₂Te₃-Cu-AlO, as shown in **Figure 1**. The multilayer structure

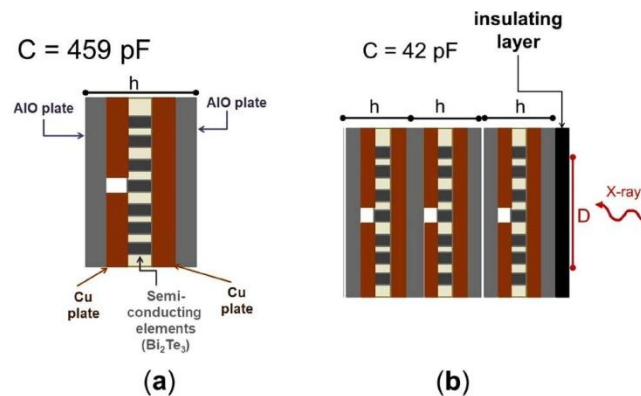


Figure 1. (a) Cross section of one simple capacitor, a single Custom Thermoelectric 07111-9L31-04B module, consisting of a layer of Bi₂Te₃ semiconducting elements embedded between alumina (AlO) and Cu plates. This module features a capacitance $C = 459 \text{ pF}$; (b) Illustration of the capacitor used in this research and consisting of three Custom Thermoelectric 07111-9L31-04B modules in series with insulating tape (IT) on the face exposed to the X-rays, which enables $C = 42 \text{ pF}$. The IT consists of heavy cotton-cloth pressure sensitive tape with strong adhesive and tensile properties. In both panels (a) and (b) the capacitance C is evaluated for the area of the capacitor exposed to the X-rays.

of each module, and the in-series combination of three of them, makes the overall device comparable to a capacitor [5]. In addition, placing an insulating layer on the face directly exposed to the X-rays, enables an equivalent capacitance C of

$\sim 42 \text{ pF}$ within the X-ray's beam size of 4 cm^2 . The value ϵ of the dielectric constant is $\epsilon = 1.423$, as computed from

where $\epsilon_0 = 8.854 \times 10^{-12} \text{ Fm}^{-1}$ is the permittivity in vacuum.

We also used a 89 pF capacitor, which we built by assembling two Custom Thermoelectric 07111-9L31-04B modules and a 07111-5L31-03CJ module. The value ϵ of the dielectric constant in this case is $\epsilon \approx 2$.

In our experiments, we assume the value of the capacitance C to be constant both in time, space, and for all frequencies of the EM waves. During the illumination with the X-rays, the capacitor is kept within two expanded polystyrene (EPS) enclosures to shield it from background noise.

Data Acquisition: Using Keithley 2000 multi-meters, capable of reading direct current (DC) voltages from 100 nV to 1 kV, we acquired the voltage difference $\Delta V(t)$ and the temperature $T_{\text{hot}}(t)$ as a function of time t . We measured $T_{\text{hot}}(t)$ using OMEGA type J self-adhesive thermocouple probes. The data collection lasted 50 minutes. During the first 30

minutes, called the *relaxation interval*, the data points were collected at low rate (one per minute) to monitor the relaxation of the capacitor in the EPS enclosures without exposure to the X-rays. During the final 20 minutes, called the *illumination interval*, the data collection under X-ray bombardment occurred at an increased rate (two per second) to visualize the effects on $\Delta V(t)$ and $T_{\text{hot}}(t)$ of five 120 s long X-ray pulses. We allowed a time interval of three minutes between one pulse and the next. In both the *relaxation* and the *illumination intervals*, we contemporarily collected $\Delta V(t)$ and $T_{\text{hot}}(t)$ using LabView 2012 and a National Instruments PXI-1042q communications chassis. We used OriginPro 2018 for analyzing the data.

3. Results

The trends in time of $T_{\text{hot}}(t)$ and $\Delta V(t)$ collected versus time from the 42 pF capacitor with and without the 40 keV X-ray illumination are shown in **Figure 2(a)** and **Figure 2(b)**, respectively. We identify two intervals in the graphs. The first corresponds to the *relaxation interval*, in which the 42 pF capacitor is not exposed to the 40 keV X-rays. The second interval corresponds to the *illumination interval*, which describes the evolution of $T_{\text{hot}}(t)$ and $\Delta V(t)$ upon exposing the 42 pF capacitor to five 120 s long X-rays pulses.

We observe that, in the *relaxation interval*, approximately 20 minutes after starting the data collection, $T_{\text{hot}}(t)$ rises, followed about 10 minutes later by the rise of $\Delta V(t)$. We ascribe the rise of both $T_{\text{hot}}(t)$ and ΔV without X-rays to background noise, which affects the 42 pF capacitor probably due to the insufficient shielding offered by the EPS enclosures. To mitigate the influence of background

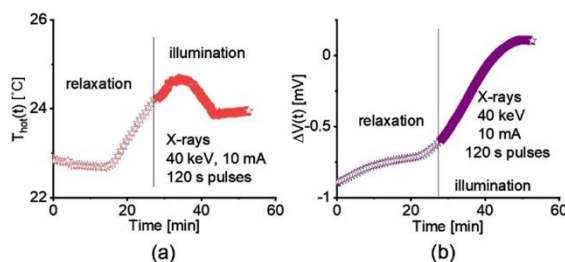


Figure 2. Trends versus time of (a) the temperature $T_{\text{hot}}(t)$ on the face of the 42 pF capacitor facing the X-ray source, and of (b) the voltage difference $\Delta V(t)$ produced by the capacitor during the whole 50 minute long experiment. During the first 30 minutes, the *relaxation interval*, the 42 pF capacitor relaxes inside two expanded polystyrene (EPS) enclosures. This interval corresponds to less dense data points. In the following 20 minutes, the *illumination interval*, the 42 pF capacitor receives five 120 s long 40 keV X-ray pulses. This interval corresponds to more dense data points.

noise, in the data analysis process we subtract the background from the acquired $T_{\text{hot}}(t)$ and $\Delta V(t)$ data.

Figure 3 focuses on three zones in the *illumination interval* exhibiting the response versus time t of the 42 pF capacitor to 120 s long exposures to the 40 keV X-rays. The responses of $T_{\text{hot}}(t)$ and $\Delta V(t)$ are shown after background subtraction. The top row of **Figure 3** (panels (a), (c) and (e)) reports the trend in time of $T_{\text{hot}}(t)$, while the bottom row (panels (b), (d) and (f)) reports those for $\Delta V(t)$. We observe that the 40 keV X-rays cause a blip in both $T_{\text{hot}}(t)$ and $\Delta V(t)$. In all three cases, the blip of T_{hot} is pronounced and relatively narrow, confined within the 120 s exposure time to the X-rays. The amplitude ΔT_{hot} of the blip in T_{hot} varies between 0.045°C and 0.1°C , and its average value is $(0.065 \pm 0.030)^\circ\text{C}$. On the other hand, in all three cases, the blip in voltage ΔV is pronounced but rather broad, rising at the beginning of the illumination pulse and declining at the end of it. The amplitude of the blip in voltage ΔV varies between $2.5 \mu\text{V}$ and $5 \mu\text{V}$, with an average value of $(3.5 \pm 1.3) \mu\text{V}$. The ratio R between the amplitudes of the blips in ΔV and ΔT_{hot} is on average $(0.055 \pm 0.005) \text{ mV}/^\circ\text{C}$ for the three examined pulses. This value is two orders of magnitude lower than the R value found in the interaction between capacitors and visible light ($R = 3.7 \pm 0.2 \text{ mV}/^\circ\text{C}$ with green light) and IR light ($R = 21.5 \pm 3.8 \text{ mV}/^\circ\text{C}$) [5]. Since the R value seems to decrease with increasing frequency ν (decreasing period τ), we find perfectly acceptable the low value of R under X-ray illumination in our ex-

periment.

Figure 4 focuses on three 120 s long zones in the *illumination interval* in which the 42 pF capacitor is not exposed to the 40 keV X-rays. In all panels, the responses of $T_{\text{hot}}(t)$ and $\Delta V(t)$ versus time t are presented without background subtraction. The top row of **Figure 4** (panels (a), (c) and (e)) illustrates $T_{\text{hot}}(t)$, while the bottom row (panels (b), (d) and (f)) displays $\Delta V(t)$. In all panels, $\Delta V(t)$ increase linearly versus time, without blips. However, in panel (f), $\Delta V(t)$ bends because it falls precisely where in the *illumination interval* $\Delta V(t)$ achieves the plateau, visible in the top-right corner of **Figure 2(b)**. On the other hand, $T_{\text{hot}}(t)$

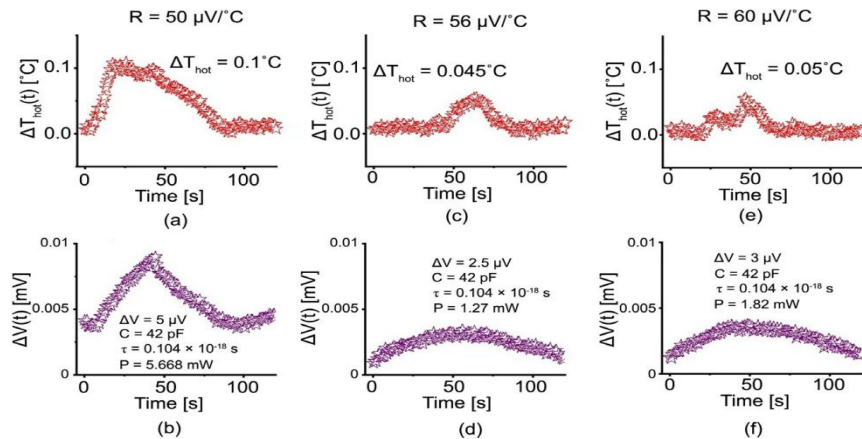


Figure 3. Zoom into three zones of $T_{\text{hot}}(t)$ and $\Delta V(t)$ in the *illumination interval* of **Figure 2**, corresponding to exposure of the 42 pF capacitor to a 120 s long pulse of 40 keV X-ray (period $\tau = 0.104 \times 10^{-18}$ s). Panels (a), (c) and (e) show, after background subtraction, the trend in time of $T_{\text{hot}}(t)$ measured on the exposed face of the 42 pF capacitor. Panels (b), (d) and (f) illustrate, after background subtraction, the corresponding voltage difference $\Delta V(t)$ in the same time zones. For each pulse, we indicate the amplitudes of the blips in T_{hot} , ΔT_{hot} , and voltage ΔV , the estimated magnitude of the average power P of the X-rays, and the R ratio (*i.e.* the ratio between ΔV and ΔT_{hot}).

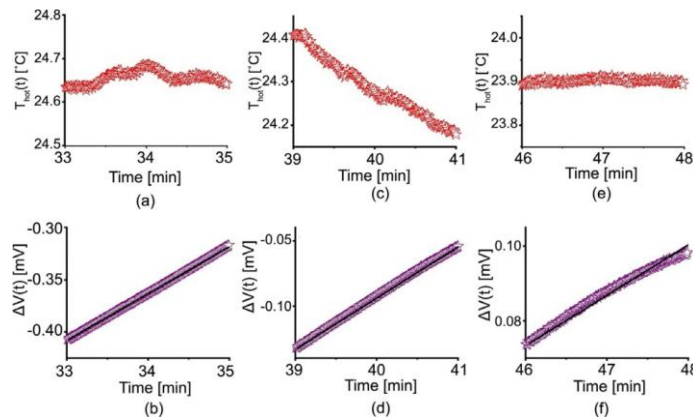


Figure 4. Zoom into three time zones of $T_{\text{hot}}(t)$ and $\Delta V(t)$ in the *illumination interval* of **Figure 2** in which the 42 pF capacitor is not exposed to X-ray pulses. Panels (a), (c) and (e) show, without background subtraction, the trends of $T_{\text{hot}}(t)$. Panels (b), (d) and (f) illustrate, without background subtraction, the corresponding voltage difference $\Delta V(t)$ in the same time zones. In panel (c) decreases linearly versus time, whereas it is flat in panel (e). Only panel (a) shows a blip of about 0.05°C , *i.e.* of the same order of magnitude of the blips detected upon exposure of the 42 pF capacitor to the 40 keV X-rays in **Figure 3**. The origin of this blip in $T_{\text{hot}}(t)$, visible in **Figure 4(a)**, is for the moment, uncertain. Overall, the comparison between **Figure 3** and **Figure 4**, considering that no background subtraction was applied to the data in **Figure 4**, suggests that the blips in $\Delta V(t)$ found in **Figure 3(b)**, **Figure 3(d)** and **Figure 3(f)** are a consequence of the 120 s long exposure of the 42 pF capacitor to the 40 keV X-rays.

Previous research [5] used the law of conservation of energy to quantify the energy involved in the interaction between

EM waves and a capacitor. The law of conservation of energy is expressed in the following equation:

$$P\tau = \frac{1}{2} C \Delta V^2 + \frac{1}{2} q^2 - \Sigma_0 \Delta T \quad (1)$$

More details about the derivation of this equation are provided in the Appendix. In Equation (1), $P\tau$ is the total energy conserved in the interaction between EM waves and a capacitor. The variables C and ΔV are, respectively, the capacitance of the capacitor, and the amplitude of the blip in voltage generated by the EM waves interacting with the capacitor. The variable q , in the second addend of Equation (1), is the amount of charge displaced by the EM waves upon their arrival on the surface of the capacitor [5]. Finally, in the third addend of Equation (1), the variable ΔT is the amplitude ΔT_{hot} of the blip of the temperature T_{hot} , and Σ_0 is entropy. All addends in Equation (1) are required to be of the same order of magnitude of $P\tau$, and vice-versa, in order to be significant. Otherwise, if they are too small they are neglected, if they are too big they prevail. A similar use of constraints is employed by the authors of Ref. [12] to estimate the surface magnetic field of the red dwarf emitting radio waves.

Here we apply Equation (1) to the interaction between X-rays and a capacitor to determine the average power P of the X-rays. To this end, we exploit the constraint that all addends in Equation (1) must be of the same order of magnitude of $P\tau$, and vice-versa, to be significant. This constraint enables us to estimate P as:

$$P \sim \frac{1}{2} C \Delta V^2 \quad (2)$$

The values of P we found using Equation (2) for the three pulses in Figure 3 are summarized in Table 1. On average, the power of the 40 keV X-rays is

Table 1. Amplitude of three blips in voltage ΔV measured during the illumination of a 42 pF capacitor with a 2 minute long 40 keV X-rays pulse. The three blips are depicted in Figure 3, panels (b), (d), and (f). Average power P of the 40 keV X-rays pulse hitting the 42 pF capacitor estimated using Equation (2). The average value of P is (2.96 ± 2.40) mW. Finally, voltage responsivity $\pi_v = \Delta V/P$ estimated for the three blips in voltage ΔV depicted in Figure 3, panels (b), (d), and (f). The average value of π_v is $(1.50 \pm 0.56) 10^{-3}$ V/W.

Panel in Figure 3	ΔV [μ V]	Average Power P [mW]	Responsivity π_v [10^{-3} V/W]
(b)	5	5.67	0.88
(d)	2.5	1.27	1.97
(f)	3	1.82	1.65

$P = (2.96 \pm 2.40)$ mW. Interestingly, this value of power is within the range (from 3 μ W to 20 mW) measured for synchrotron X-rays [15]. This observation suggests that the value we have found is reasonable. Knowing P , we estimate the average value of the total energy as $P\tau = 0.31 \times 10^{-21}$ J. Proceeding in the same way from Equation (1), and using the average value of the amplitude of the blip in T_{hot} ($0.065^\circ\text{C} \pm 0.030^\circ\text{C}$), we determine the average value of the entropy Σ_0 as $\sim 4.7 \times 10^{-21}$ J/ $^\circ\text{C}$. Similarly, since the capacitance C of the capacitor is 42 pF, the displaced charge q in Equation (1) is estimated to be of the order of $\sim 1.61 \times 10^{-16}$ C.

4. Discussion

In our experiment, two routes help assessing whether $P\tau$ is the total energy conserved in X-ray absorption. Both routes

exploit the average power $P = 2.96$ mW that we estimated through $P\tau$ and the law of conservation of energy. The first route verifies that $P = 2.96$ mW supports the performance of the standard medical X-ray imaging machine we used in our experiment. The second route compares with trends established for other EM waves, the voltage responsivity π_V [5] imposed by $P = 2.96$ mW on the 42 pF capacitor [5]. Indeed, predictions involving a broad range of EM waves indicate that the voltage responsivity π_V generated in capacitors decreases by several orders of magnitude under illumination with EM waves of increasing frequency ν (or decreasing period τ , or wavelength λ). Radio waves are expected to yield larger voltage responsivities than IR and visible light [5]. We thus expect the voltage responsivities generated by X-rays to be smaller than those generated by the other EM waves, in particular visible and IR light, and radio waves.

4.1. The X-Ray Power in a Standard X-Ray Imaging Medical Machine

Power-meters responsive to visible light easily allow measuring the power of an optical laser beam. Unfortunately, power meters responsive to X-rays are at the infancy of their development and, to date, are only in use for research purposes

[15] [16]. Usually these power meters are large, heavy, operating at low temperatures and difficult to operate. Even if compact and easy-to-use X-ray power-meters are available [15], neither power nor intensity (power per area) are operating parameters in standard medical X-ray imaging machines. Rather, these machines are set to deliver an effective dose (Δ_{eff} , in units of Sv, Sievert, or J

* kg^{-1}) of X-rays on a specific patient's organ. The effective dose Δ_{eff} establishes the energy $E_{\text{abs}} = \Delta_{\text{eff}} m$ to be absorbed by the mass m within the organ to obtain the desired imaging or therapeutic goal. We call E_{abs} the transferred energy, which differs from the total energy $P\tau$. Specifically, the transferred energy E_{abs} is the amount of energy transferred to the mass m in a selected volume V independently of the exposure time Δt . Instead, the total energy $P\tau$ corresponds to the amount of energy transferred within the period τ of the EM wave in the volume of matter hit by the EM wave. Analogously to Equation (1), we hypothesize that the total energy $P\tau$ and the transferred energy E_{abs} are related through the law of conservation of energy such that:

$$\frac{P\tau}{\Delta t} = \tau \Delta$$

or

$$m - \sum_0 \Delta T$$

$$P\tau = E_{\text{abs}} - \sum_0 \Delta T \quad (3)$$

Δt

As in Equation (1), also in Equation (3) all addends, to be significant, are required to be of the same order of magnitude of $P\tau$. Therefore, we can approximate Equation (3) as follows:

$$\frac{P\tau}{\Delta t} \sim \tau \Delta \quad (4)$$

Knowing both the mass m and the exposure time Δt , this approximation allows us to constrain the value of the average power P of the X-rays from the known value of the dose Δ_{eff} . For instance, for a typical mammogram, $\Delta_{\text{eff}} = 0.36 \text{ mSv}$ or $0.36 \text{ mJ} \cdot \text{kg}^{-1}$ [17]. The density of the breast tissue is, on average, $\delta = 0.985 \text{ g/cm}^3$. Therefore, a volume $V = 9 \text{ cm}^3$ (diameter $d = 1.3 \text{ cm}$) of breast tissue has a mass m of about $8.86 \times 10^{-3} \text{ kg}$. The transferred energy $E_{\text{abs}} = \Delta_{\text{eff}} m$ from the X-rays to the breast tissue, is therefore $3.19 \times 10^{-6} \text{ J}$, and an exposure time $\Delta t = 1.1 \text{ ms}$ would be compatible with the average power $P = 2.96 \text{ mW}$ found with $P\tau$ and the law of conservation of energy in Section 3. Similarly, with $\Delta t = 0.2 \text{ s}$, which is the exposure time normally adopted in mammogram screenings, and assuming an average power $P = 2.96 \text{ mW}$, a breast tissue volume V with a diameter $d = 12 \text{ cm}$ could be imaged. Thus, either $V = 9 \text{ cm}^3$ ($d = 1.3 \text{ cm}$) and $\Delta t = 1.1 \text{ ms}$, or $d = 12 \text{ cm}$ and $\Delta t = 0.2 \text{ s}$, represent realistic scenarios. From these examples, we

conclude that the X-ray's average power estimated as P

$= 2.96 \text{ mW}$ satisfies the expectations on the performance of a standard medical X-ray imaging machine.

An additional example consists of using the X-rays of our standard medical machine to image wrist and hand bones.

In this case, $\Delta_{\text{eff}} = 4 \text{ mSv}$ [17], and $\delta =$

1.92 g/cm^3 . Thus, for $V = 9 \text{ cm}^3$ ($d = 1.3 \text{ cm}$), m is $17.3 \times 10^{-3} \text{ kg}$, which determines a transferred energy $E_{\text{abs}} = 69.1 \times 10^{-6} \text{ J}$. In this condition, an exposure time $\Delta t = 0.02 \text{ s}$ is compatible with the average power $P = 2.96 \text{ mW}$. If we instead choose $\Delta t = 0.2 \text{ s}$ while $P = 2.96 \text{ mW}$, we could image a wrist or hand bone volume of diameter $d = 4 \text{ cm}$. Both scenarios are realistic, thus we conclude that also in imaging wrist and hand bones the average power $P = 2.96 \text{ mW}$ satisfies the expectations on the performance of a standard medical X-ray imaging machine.

Summarizing, in Section 3, using the total energy $P\tau$ and the law of conservation of energy, we estimate the average power of the X-rays from a machine previously used for medical imaging to be $P = (2.96 \pm 2.40) \text{ mW}$. Subsequently, in Section 4.1, using the concept of transferred energy, we find that the average power $P = 2.96 \text{ mW}$ is compatible with the X-ray exposure time Δt typically applied to image patient's organs. This result validates our approach for estimating the power of an X-ray beam with $P\tau$ and the law of conservation of energy.

4.2. The Responsivity π_V of the 42 pF Capacitor under X-Ray Illumination

Responsivity is a parameter used to characterize the performance of devices such as sensors, detectors and energy harvesters under the effect of EM waves [18]. Analytically, responsivity is the ratio between the change in voltage, or current, produced by the specific device, and the power P of the EM wave that illuminates the device. For example, when the device produces a voltage change ΔV , the voltage responsivity is $\pi_V = \Delta V/P$. Similarly, when the device produces a current change ΔI , the current responsivity is $\pi_I = \Delta I/P$.

Using $P\tau$ and the law of conservation of energy, Boone *et al.* [5] found that the voltage responsivity $\pi_V = \Delta V/P$ of capacitors illuminated by visible and IR light decreases with decreasing period τ of the EM waves. In other words, the capacitor's responsivity π_V is lower for visible than for IR light excitation. Consequently, we expect π_V to be even lower with X-ray illumination of a capacitor. Our goal is to verify that, based upon the X-ray's average power $P = 2.96 \text{ mW}$ found in our experiment (Section 3), the voltage responsivity π_V of the capacitors illuminated by X-rays is lower than that produced under visible and IR light exposure. Thus, we evaluate π_V by dividing the ΔV values in Figure 3, panels (b), (d), and (f) to the corresponding values of P , as summarized in Table 1. We report the voltage responsivity π_V values in Table 1, and estimate their average to be $(1.50 \pm 0.56) \times 10^{-3} \text{ V/W}$. With visible and IR light in the $\lambda = 532 \text{ nm}$ to 2000 nm wavelength range, or period range between $1.77 \times 10^{-15} \text{ s}$ to $6.67 \times 10^{-15} \text{ s}$, the voltage responsivity π_V varies between 2×10^{-2} to $2 \times 10^{-1} \text{ V/W}$ on a 18 pF capacitor [5]. These values are one to two orders of magnitude larger than $1.50 \times 10^{-3} \text{ V/W}$. Since the difference in capacitance between 18 and 42 pF is small, we can safely state that the voltage responsivity π_V of capacitors exposed to X-rays is lower, by at least one order of magnitude, than that produced by capacitors illuminated with visible and IR light. We therefore conclude that the voltage responsivity π_V in our experiment with X-rays behaves as predicted in Ref. [5].

In Figure 5 and Table 2 we illustrate the trend of the voltage responsivity π_V from X-rays (this research) to visible and IR light (Ref. [5]) by showing π_V as a function of the period τ of the EM waves. In Figure 5 π_V , which spans over thirteen orders of magnitude, appears on a logarithmic scale on the y-axis. The x-axis, also in logarithmic scale, covers thirteen orders of magnitude of the period τ . We include in the figure our preliminary data taken with radio waves, and fit the experimental points with the function $\pi_V \approx 1 \times 10^{14} \tau \text{ C}^{-1}$ (here $\text{C} = \text{Coulomb}$). The datum corresponding to the illumination with the 40 keV X-ray pulses is marked as "pulsed". This point is rather above the fitting line because of the weakness of the voltage signal generated. The datum that falls on the fitting line corresponds to measurements taken with continuous wave (cw) X-rays (data discussed below). Despite the uncertainties, we conclude that the trend,

Table 2. Comparison of ratio R (ratio between the amplitudes of the jumps of voltage ΔV and temperature ΔT_{hot}), average power P , energy $P\tau$, entropy Σ_0 , charge q , and voltage responsivity π_V involved in the interaction with a capacitor of 40 keV X-rays (this research), Cu K- α and - β X-rays (this research), visible and infrared (IR) light (Ref. [5]). The trend of the voltage responsivity π_V over the range from X-rays to IR light is further illustrated in **Figure 5**.

	40 keV X-rays ($\tau = 0.104 \times 10^{-18}$ s), this research		
	Cu K- α and - β X-rays($\tau \sim 0.51 \times 10^{-18}$ s), this research		
	visible and infrared light (from 1.77×10^{-15} s to 3.55×10^{-15} s), Ref. [5]		
R (mV/ $^{\circ}\text{C}$)	0.055	0.8	from 3.7 ± 0.2 to 21.5 ± 3.8
average power P (mW)	2.96 (calculated)	14800 (calculated)	from 25 to 700 (experimental)
	3.11×10^{-22}	7.55×10^{-18}	$\sim 9.64 \times 10^{-16}$
Σ_0 (entropy, J/ $^{\circ}\text{C}$)	4.7×10^{-21} (calculated)	1.45×10^{-17} (calculated)	$\sim 10^{-16}$
q (charge, C)	1.61×10^{-16} (calculated)	3.7×10^{-14} (calculated)	$\sim 10^{-12}$
π_V (voltage responsivity mV/W)	1.5	0.028	from 20 to 200

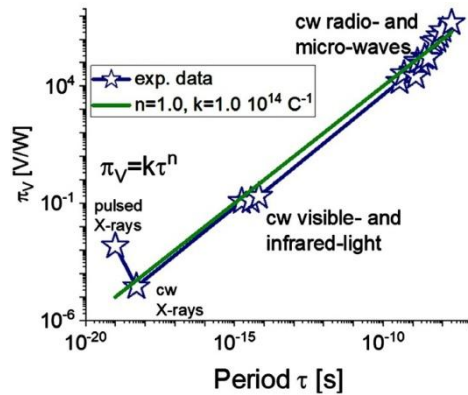


Figure 5. Trend versus electromagnetic (EM) wave's period τ of the voltage responsivity $\pi_V = \Delta V/P$ of capacitors illuminated by radio waves (preliminary data), infrared (IR) [5], visible [5], and X-rays (this research). The magnitudes of π_V are summarized in **Table 2**. The x-axis, in logarithmic scale, covers thirteen orders of magnitude of the period τ , while the y-axis, also in logarithmic scale, spans over thirteen orders of magnitude of the voltage responsivity π_V . The experimental data points are fitted with the function $\pi_V \approx 1 \cdot 10^{14} \tau \text{ C}^{-1}$ (here $\text{C} = \text{Coulomb}$). Most of the data points were taken from illumination with continuous EM waves (cw). The datum generated by the 40 keV X-ray pulses is marked as "pulsed".

detected in **Figure 5**, of the voltage responsivity π_V of capacitors exposed to X-rays also validates our approach to estimate the power of an X-ray beam with $P\tau$ and the law of conservation of energy.

4.3. Additional Assessment through the Illumination of an 89 pF Capacitor with Cu K- α and - β X-Rays

To further assess the ability of our procedure to effectively measure the average power P of X-rays, we exposed a 89 pF capacitor to Cu K- α and - β X-rays obtained from a powder X-ray diffractometer (PXRD) (X'pert PANalytical). We built the 89 pF capacitor by assembling two Custom Thermoelectric 07111-9L31-04B modules and a 07111-5L31-03CJ module. The X-rays have an average wave-

length $\lambda \sim 1.5406 \times 10^{-10}$ m, average frequency $\nu \sim 1.947 \times 10^{18}$ Hz, and average period $\tau \sim 0.51 \times 10^{-18}$ s. We directed the X-rays normally to the capacitor's surface for about 20 minutes. Due to the impossibility of contemporarily fit three multi-meters in the housing of the X'pert PANalytical X-ray diffractometer, we asynchronously measured the trends in time of the voltage $\Delta V(t)$ and temperature $T_{\text{hot}}(t)$, shown in **Figure 6**. The jumps of $\Delta V(t)$ and $T_{\text{hot}}(t)$ are well defined, and the data do not demand a background subtraction. We observe an amplitude of the jumps in voltage and temperature of $\Delta V = 0.41$ mV and $\Delta T_{\text{hot}} = 0.52^\circ\text{C}$, respectively. From these amplitudes, and using a procedure similar to that adopted in Section 3 and Section 4.1, we estimate the ratio R between the amplitudes of the jumps of ΔV and ΔT_{hot} , the average power P , the total energy $P\tau$, the entropy Σ_0 , the displaced charge q , and the voltage responsivity π_V . These results are summarized in **Table 2**, where the quantities are compared to the corresponding ones obtained with the 40 keV X-rays (this research) and with visible and IR light (Ref. [5]). From these comparisons, we observe that the values of R produced by capacitors illuminated with X-rays are significantly smaller than those generated by capacitors exposed to visible and IR lights. This finding indicates that relatively larger temperature differences arise from the interaction of capacitors with EM waves at higher frequencies than at lower frequencies. This observation correlates with the finding that X-rays require a large value of average power P to give rise to even a small change in voltage ΔV , as inferred from the low values of the voltage responsivities π_V in **Table 2**. Consequently, in standard medical X-ray imaging machines, P needs to be set at the lowest possible value to avoid danger for patients and operators, in agreement with our findings in Section 4.1. Finally, the value of the total energy $P\tau$ and Equation (1) enable us to compute the entropy Σ_0 and the displaced charge q , as reported in **Table 2**.

One striking characteristics of the energy $P\tau$ emerging from **Figure 6** needs further comments. The jump in voltage ΔV caused by the Cu K- α and - β X-rayson the 89 pF capacitor is of the same order of magnitude of that generated at

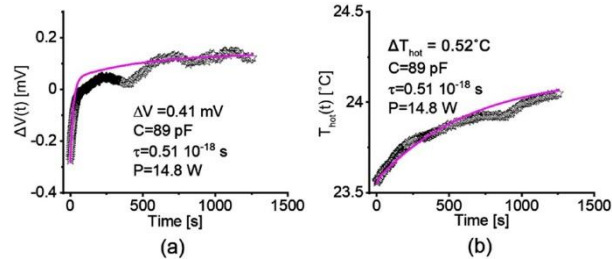


Figure 6. Trends versus time of (a) $\Delta V(t)$ and (b) $T_{\text{hot}}(t)$ generated by the illumination of a 89 pF capacitor with Cu K- α and - β X-rays (period $\tau = 0.51 \cdot 10^{-18}$ s). The trends were measured asynchronously, due to the impossibility to contemporarily fit three multi-meters in the housing of the X'pert PANalytical X-ray diffractometer used for the experiment. No background subtraction is necessary in these data sets. In each panel, we indicate the amplitudes of the jumps in voltage ΔV and temperature ΔT_{hot} , and the estimated magnitude of the average power P of the X-rays.

much lower average power P by green light from Ref. [5], and radio waves from our preliminary data. The result is depicted in **Figure 7** and **Table 3**. The corresponding values of $P\tau$ in the three cases turn out to be of the same order of magnitude. This observation suggests that waves with the same total energy $P\tau$ produce similar effects, e.g. the same jump in voltage ΔV . Therefore, since X-rays have smaller values of the period τ than, e.g. visible light, it turns out that X-rays achieve the same energy $P\tau$ of visible light with larger values of average power P than visible light. Accordingly, the effects of the average power $P \sim 3$ mW of X-rays with period $\tau = 1 \times 10^{-19}$ s produced by our standard medical X-ray imaging machine and generating a $P\tau = 3 \times 10^{-22}$ J, are the same as those due to green light at $\tau = 1.77 \times 10^{-15}$ s with average power $P \sim 1.69 \times 10^{-7}$ W!

5. Conclusions

In this research, we explore the interaction between X-rays and a capacitor. We achieve the following conclusions: 1) The

product of the average power P times, the period τ , i.e. $P\tau$, is the total energy conserved in the absorption process also

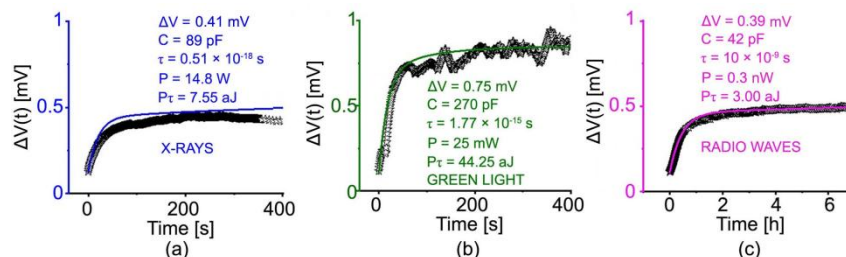


Figure 7. Trends in time of the voltage difference $\Delta V(t)$ generated through the illumination of capacitors with various values of capacitance C , by Cu K- α and - β X-rays (a); green light (b); and radio waves (c). The period τ and the average power P of the various electromagnetic (EM) waves, and the values of the jumps in voltage ΔV are indicated in each panel. We highlight that the values of ΔV and $P\tau$ are of the same order of magnitude in the three cases (see Table 3 for numerical details).

Table 3. Summary of the similar experimentally measured jumps of voltage ΔV of about (0.51 ± 0.20) mV produced on a capacitor of capacitance C by electromagnetic (EM) waves of period τ , average power P , and total energy $P\tau$ (average value 18.3 ± 22.6 J). As EM waves for this summary, we have chosen Cu K- α and - β X-rays from this research, green light from Ref. [5], and radio waves from our preliminary data. The experimental trends of $\Delta V(t)$ under illumination of the capacitor by Cu K- α and - β X-rays, green light, and radio waves are summarized in Figure 7.

	Cu K- α and - β X-rays, this research	Green light, Ref. [5]	Radio waves, preliminary data
ΔV (mV)	0.41	0.75	0.39
C (pF)	89	270	42
τ (s)	0.51×10^{-18}	1.77×10^{-15}	10×10^{-9}
P (W)	14.8	25×10^{-3}	0.3×10^{-9}
$P\tau$ (aJ)	7.55	44	3

for X-rays, not just for visible and infrared (IR) lights. 2) The voltage responsivity of the capacitor decreases with increasing frequency ν (or decreases with decreasing period τ) of the electromagnetic (EM) waves. Indeed, the voltage responsivity π_ν of the capacitor we used in our investigation is significantly smaller than that previously determined by illumination with visible and IR light of the same capacitor. 3) The formalism related to $P\tau$ and the law of conservation of energy enables us to unveil the relationship between the average power P of the X-rays and the effective dose delivered on an organic sample. The effective dose is an important operating parameter in standard medical imaging machines employing X-rays.

In addition to these fundamental results, we achieve a significant practical result: the procedure we used in our investigation enables us to measure the average power P of the X-rays generated in two machines, one originally designed for usage in medical imaging, and the other designed for X-ray diffraction of powders. The power P is of the order of few mW for the standard X-ray medical imaging machine, and W for the X-ray diffractometer. Our procedure paves the ground for designing an X-ray power-meter, a tool presently missing in the market of X-ray characterization tools.

Acknowledgements

This work was supported by the JMU Department of Physics and Astronomy, and the JMU Center for Materials Science. The authors thank A. Banu and S. Pendleton for fruitful discussions and for technical support at the Madison Accelerator Laboratory (JMU). The authors also thank B. A. Reisner and X. Hu (JMU, Chemistry and Biochemistry) for technical support, and gratefully acknowledge the National Science Foundation (NSF) for

instrumentation support(DMR-0315345) enabling the X-Ray measurement performed with the X-ray diffractometer (PXRD) (X'pert PANalytical). Any opinions, findings, and conclusions or recommendations expressed in this material are those of the authors and do not necessarily reflect the views of the NSF.

Conflicts of Interest

The authors declare no conflicts of interest regarding the publication of this paper.

References

- [1] Field, G.D. and Rieke, F. (2002) Nonlinear Signal Transfer from Mouse Rods to Bi-polar Cells and Implications for Visual Sensitivity. *Neuron*, **34**, 773-785. [https://doi.org/10.1016/S0896-6273\(02\)00700-6](https://doi.org/10.1016/S0896-6273(02)00700-6)
- [2] Osterhoudt, G.B., Diebel, L.K., Gray, M.J., Yang, X., Stanco, J., Huang, X., Shen, B., Ni, N., Moll, P.J., Ran, Y. and Burch, K.S. (2019) Colossal Mid-Infrared Bulk Photovoltaic Effect in a Type-I Weyl Semimetal. *Nature Materials*, **18**, 471-475. <https://doi.org/10.1038/s41563-019-0297-4>
- [3] Ji, Z., Liu, G., Addison, Z., Liu, W., Yu, P., Gao, H., Liu, Z., Rappe, A.M., Kane, C.L., Mele, E.J. and Agarwal, R. (2019) Spatially Dispersive Circular Photogalvanic Effect in a Weyl Semimetal. *Nature Materials*, **18**, 955-962. <https://doi.org/10.1038/s41563-019-0421-5>
- [4] Rivera, N., Wong, L.J., Joannopoulos, J.D., Soljačić, M. and Kaminer, I. (2019) Light Emission Based on Nanophotonic Vacuum Forces. *Nature Physics*, **15**, 1284-1289. <https://doi.org/10.1038/s41567-019-0672-8>
- [5] Boone, D.E., Jackson, C.H., Swecker, A.T., Hergenrather, J.S., Wenger, K.S., Kokhan, O., Terzić, B., Melnikov, I., Ivanov, I.N., Stevens, E.C. and Scarel, G. (2018) Probing the Wave Nature of Light-Matter Interaction. *World Journal of Condensed Matter Physics*, **8**, 62-89. <https://doi.org/10.4236/wjcmp.2018.82005>
- [6] Gordon, A.L. and Scarel, G. (2018) Interaction in the Steady State between Electromagnetic Waves and Matter. *World Journal of Condensed Matter Physics*, **8**, 171-184. <https://doi.org/10.4236/wjcmp.2018.84012>
- [7] Scarel, G. and Stevens, E.C. (2019) The Effect of Infrared Light's Power on the Infrared Spectra of Thin Films. *World Journal of Condensed Matter Physics*, **9**, 1-21. <https://doi.org/10.4236/wjcmp.2019.91001>
- [8] Scarel, G. (2019) Quantum and Non-Quantum Formulation of Eye's Adaptation to Light's Intensity Increments. *World Journal of Condensed Matter Physics*, **9**, 62-74. <https://doi.org/10.4236/wjcmp.2019.93005>
- [9] Scarel, G. (2019) The Role of π in the Photothermoelectric Effect and in Photoredox Catalysis Reactions. *World Journal of Condensed Matter Physics*, **9**, 91-101. <https://doi.org/10.4236/wjcmp.2019.94007>
- [10] Yan, W., Frühling, C., Golovin, G., Heden, D., Luo, J., Zhang, P., Zhao, B., Zhang, J., Liu, C., Chen, M., Chen, S., Banerjee, S. and Umstadter, D. (2017) High-Order Multiphoton Thomson Scattering. *Nature Photonics*, **11**, 514-520. <https://doi.org/10.1038/nphoton.2017.100>
- [11] Pickens, K.T. and Scarel, G. (2020) Estimation of the Power of the Anomalous Microwave Emission. *World Journal of Condensed Matter Physics*, **10**, 105-117. <https://doi.org/10.4236/wjcmp.2020.103007>
- [12] Vedantham, H.K., Callingham, J.R., Shimwell, T.W., Tasse, C., Pope, B.J., Bedell, M., Snellen, I., Best, P., Hardcastle, M.J., Haverkorn, M., Mechev, A., O'Sullivan, S.P., Röttgering, H.J.A. and White, G.J. (2020) Coherent Radio Emission from a Quiescent Red Dwarf Indicative of Star-Planet Interaction. *Nature Astronomy*, **4**, 577-583. <https://doi.org/10.1038/s41550-020-1011-9>
- [13] Kim, M.H., Vickers, E. and Gersdorff, H.V. (2012) Patch-Clamp Capacitance Measurements and Ca^{2+} Imaging at Single Nerve Terminals in Retinal Slices. *Journal of Visual Experiments*, **59**, e3345. <https://doi.org/10.3791/3345>
- [14] Adam, Y., Kim, J.J., Lou, S., Zhao, Y., Xie, M.E., Brinks, D., Wu, H., Mostajo-Radji, M.A., Kheifets, S., Parot, V., Chettih, S., Williams, K.J., Gmeiner, B., Farhi, S.L., Madisen, L., Buchanan, E.K., Kinsella, I., Zhou, D., Paninski, L., Harvey, C.D., Zeng, H., Arlotta, P., Campbell, R.E. and Cohen, A.E. (2019) Voltage Imaging and Optogenetics Reveal Behavior-Dependent Changes in Hippocampal Dynamics. *Nature*, **569**, 413-417. <https://doi.org/10.1038/s41586-019-1166-7>
- [15] Tanaka, T., Kato, M., Saito, N., Owada, S., Tono, K., Yabashi, M. and Ishikawa, T. (2017) Compact Bolometric Radiometer for Free-Electron Lasers in a Wavelength Range from Extreme-Ultraviolet to X-Rays. *Optics Letters*, **42**, 4776-4779. <https://doi.org/10.1364/OL.42.004776>
- [16] Heimann, P., Fritz, D., Krzywinsky, J., Moeller, S., Nordlund, D., Reid, A., Stefan, P., Walter, P. and Welch, J. (2019) Laser Power Meters as Portable X-Ray Power

Monitors. *X-Ray Free-Electron Lasers: Advances in Source Development and In-strumentation V*, **11038**, Article ID: 110380R.
<https://doi.org/10.1117/12.2526119>

- [17] (2020) Radiation Exposure from Medical Exams and Procedures. Health Physics Society Specialists in Radiation Safety, 1-4.
- [18] Zhao, D., Fabiano, S., Berggren, M. and Crispin, X. (2017) Ionic Thermoelectric Gating Organic Transistors. *Nature Communications*, **8**, Article No. 14214. <https://doi.org/10.1038/ncomms14214>
- [19] Chandler, D. (1987) Introduction to Modern Statistical Mechanics. Oxford University Press Inc., Oxford.

Appendix

To justify the use of $P\tau$ and the law of conservation of energy, we exploit the total differential dE of the energy transferred from the EM waves to the capacitor on an area A_{cs} with diameter D corresponding to the cross-section of the EM beam:

$$dE = qd\Delta V + \Delta Vdq - \Sigma d\Delta T - \Delta Td\Sigma, \quad (A1)$$

where $q = \sigma A_{cs}$ is charge, $\sigma = q/A_{cs}$ is surface charge density, and Σ is entropy.

The thermal component of Equation (A1) is preceded by a negative sign to signify that part of the energy transferred to the capacitor as electrical energy is

thermally dissipated. Hypothesizing that the capacitance C separate the terms containing q and ΔV enables us to, thus reducing Equation (A1) to:

$$dE = C\Delta Vd\Delta V + q dq - \Sigma d\Delta T \quad (A2)$$

where we assume $d\Sigma$ to be negligible. In a generalized grand-canonical ensemble [19], the entropy Σ is the Legendre transformation of Σ_0 , the entropy of the canonical ensemble, such that

$$\Sigma = \Sigma_0 - k_B \beta q \Delta V$$

[19], where $k_B = 1.38 \times 10^{-23}$ J/K

is Boltzmann's constant, and $\beta = 1/k_B T$. Therefore:

$$dE = C\Delta Vd\Delta V + q dq - \Sigma d\Delta T + k_B \beta q \Delta Vd\Delta T \quad (A3)$$

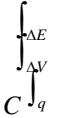
Assuming $k_B \beta q \Delta V$ to give just a slight correction to Σ_0 , dE is further reduced to:

$$dE \approx C\Delta Vd\Delta V + q dq - \Sigma d\Delta T \quad (A4)$$

At the start of the illumination of the capacitor with visible or IR light, the energy conserved in each instant of time t is $E(t) = P(t)\Delta t$. Here $P(t)$ is the exponential function that describes the rise in time of the EM wave's power with a time constant τ_P such that:

where $P_0 \approx P_{ssli} \approx P$ and P is the average power in the steady state illumination (ssli) regime. In the ssli the energy conserved is $E_c = P\Delta t$. To obtain $E(t)$ and E_c , we integrate the variables ΔV , E , q , and ΔT between their minima and maxima values:

$$\int_{q_{MAX}}^{\Delta V_{MAX}} \Delta Vd\Delta V + \int_{q_{MAX}}^{\Delta V_{MAX}} q dq - \int_{q_{MAX}}^{\Delta V_{MAX}} \Sigma d\Delta T = \int_{q_{MAX}}^{\Delta V_{MAX}} dE = C \Delta E_{MAX}$$



$$\int_0^{\Delta T}$$

min

min

min

min

We redefine the variables such that their minima are set at zero in their respective units and their maxima correspond to the values of the variables at an arbitrary instant of time t such that $\Delta V_{\text{MAX}} = \Delta V(t)$, $\Delta E_{\text{MAX}} = \Delta E(t)$, $q_{\text{MAX}} = q(t)$, and $\Delta T_{\text{MAX}} = \Delta T(t)$. The integration leads to:

$$\frac{1}{2} q(t)^2$$

$$\frac{C \Delta V(t)^2}{2} + \frac{1}{2} q(t)^2 - \Sigma \Delta T(t)$$

(A7a)

$$E(t) = P(t) \Delta t =$$

$$22 \quad C^0$$

In particular, in the ssli the integration gives:

$$\frac{1}{2} E = P \Delta t =$$

$$\frac{C \Delta V^2}{2} + \frac{1}{2} q_{\text{ssli}}^2 - \Sigma \Delta T$$

(A7b)

where q_{ssli} is the surface charge in the ssli on the area A_{cs} . Simulations show that Equation (A7) is effective if $\Delta t = \tau$, the period of the EM wave.